HHS Public Access

Author manuscript

*Cell Rep*. Author manuscript; available in PMC 2024 August 05.

Published in final edited form as:

*Cell Rep*. 2024 July 23; 43(7): 114375. doi:10.1016/j.celrep.2024.114375.

# The exocyst subunit EXOC2 regulates the toxicity of expanded GGGGCC repeats in *C9ORF72*-ALS/FTD

**Dilara O. Halim**[1,2], **Gopinath Krishnan**[1], **Evan P. Hass**[3], **Soojin Lee**[1], **Mamta Verma**[1], **Sandra Almeida**[4], **Yuanzheng Gu**[5], **Deborah Y. Kwon**[5], **Thomas G. Fazzio**[3], **Fen-Biao Gao**[1,2,4,6,*]

[1]Frontotemporal Dementia Research Center, RNA Therapeutics Institute, University of Massachusetts Chan Medical School, Worcester, MA 01605, USA

[2]Graduate Program in Neuroscience, Morningside Graduate School of Biomedical Sciences, University of Massachusetts Chan Medical School, Worcester, MA 01605, USA

[3]Department of Molecular, Cell, and Cancer Biology, University of Massachusetts Chan Medical School, Worcester, MA 01605, USA

[4]Department of Neurology, University of Massachusetts Chan Medical School, Worcester, MA 01605, USA

[5]Neuromuscular & Muscle Disorders, Biogen, Cambridge, MA 02142, USA

[6]Lead contact

## SUMMARY

GGGGCC ($G_4C_2$) repeat expansion in *C9ORF72* is the most common genetic cause of amyotrophic lateral sclerosis (ALS) and frontotemporal dementia (FTD). How this genetic mutation leads to neurodegeneration remains largely unknown. Using CRISPR-Cas9 technology, we deleted *EXOC2*, which encodes an essential exocyst subunit, in induced pluripotent stem cells (iPSCs) derived from *C9ORF72*-ALS/FTD patients. These cells are viable owing to the presence of truncated EXOC2, suggesting that exocyst function is partially maintained. Several disease-relevant cellular phenotypes in *C9ORF72* iPSC-derived motor neurons are rescued due to, surprisingly, the decreased levels of dipeptide repeat (DPR) proteins and expanded $G_4C_2$ repeats-containing RNA. The treatment of fully differentiated *C9ORF72* neurons with *EXOC2* antisense oligonucleotides also decreases expanded $G_4C_2$ repeats-containing RNA and partially rescued disease phenotypes. These results indicate that EXOC2 directly or indirectly regulates the level of $G_4C_2$ repeats-containing RNA, making it a potential therapeutic target in *C9ORF72*-ALS/FTD.



*Correspondence: fen-biao.gao@umassmed.edu.

AUTHOR CONTRIBUTIONS

Project initiation, F.-B.G. and D.O.H.; conceptualization, F.-B.G. and D.O.H.; investigations, D.O.H., G.K., E.P.H., S.L., M.V., Y.G., and D.Y.K.; formal data analysis, D.O.H., G.K., E.P.H., S.L., S.A., T.G.F., and F.-B.G.; funding acquisition, F.-B.G. and T.G.F.; supervision, F.-B.G.; writing – original draft, D.O.H.; writing – review & editing, F.-B.G., D.O.H., G.K., S.A., S.L., and T.G.F.

SUPPLEMENTAL INFORMATION

Supplemental information can be found online at https://doi.org/10.1016/j.celrep.2024.114375.

DECLARATION OF INTERESTS

The authors declare no competing interests.

## In brief

Halim et al. deleted the gene *EXOC2* from patient stem cells and then differentiated them into motor neurons. They found that several amyotrophic lateral sclerosis-related phenotypes were rescued in patient neurons when *EXOC2* was deleted or knocked down by a drug. This study identifies *EXOC2* as a potential therapeutic target.

## Graphical Abstract

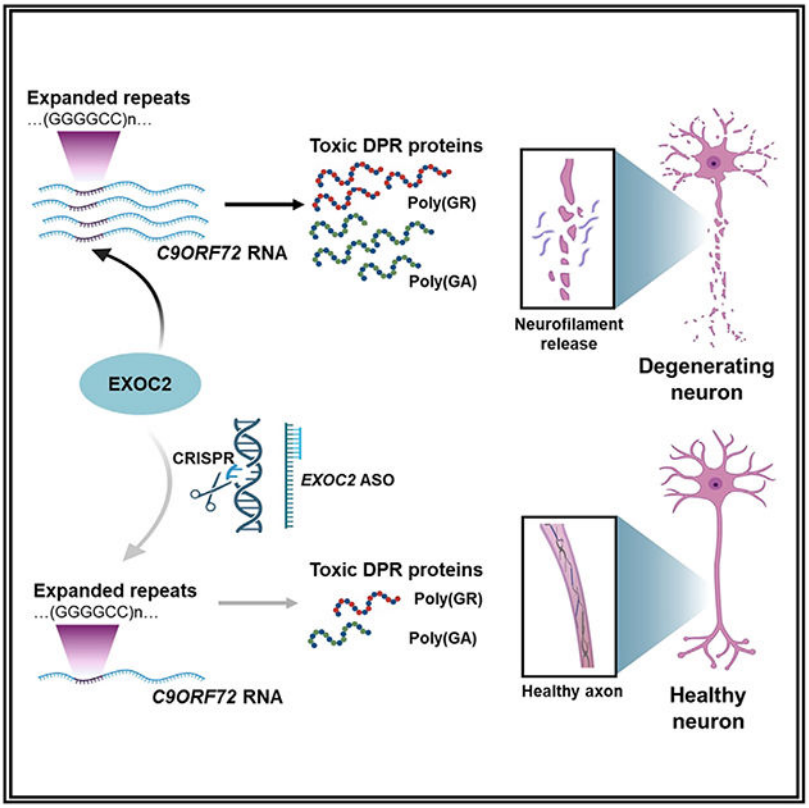


## INTRODUCTION

Amyotrophic lateral sclerosis (ALS) and frontotemporal dementia (FTD) are devastating and incurable neurodegenerative diseases that share genetic, molecular, and pathological mechanisms.[1–3] In particular, the most common genetic cause of both diseases is GGGGCC ($G_4C_2$) repeat expansion in the first intron of *C9ORF72*.[4,5] A key pathological hallmark of *C9ORF72*-ALS/FTD is the presence of five dipeptide repeat (DPR) proteins translated from expanded sense and antisense repeat RNAs: poly(GA), poly(GP), poly(GR), poly(PR), and poly(PA).[6–8] Poly(GR) expression patterns correlate with neurodegeneration in *C9ORF72* patients' brains,[9–11] and ectopic expression of poly(GR) confers strong toxicity in diverse *in vitro* and *in vivo* models.[12–19] Poly(GR) interacts with several cellular components such as ribosomes, stress granules, spliceosomes, and nucleolar proteins and impairs various cellular functions, including translation, nucleocytoplasmic transport, stress granule dynamics, splicing, mitochondrial function, DNA damage, and stress response.[15,17,20–27]

Despite this recent progress, our understanding of altered pathways in *C9ORF72*-ALS/FTD is incomplete, and we do not know which pathway(s) can be targeted therapeutically in patient neurons. In an unbiased genetic screen in poly(GR)-expressing *Drosophila*, we identified *Sec5* as a genetic suppressor of poly(GR) toxicity in non-neuronal cells.[21] Sec5/EXOC2 is a subunit of the octameric exocyst complex. Exocysts participate in protein trafficking and spatiotemporal regulation of soluble *N*-ethylmaleimide-sensitive factor attachment protein receptor (SNARE) complex assembly for exocytosis, which is essential for neuronal function and other cellular processes during development and in adulthood.[28–30]

In this study, we investigated the role of EXOC2 in the pathogenesis of *C9ORF72*-ALS/FTD in motor neurons (MNs) derived from induced pluripotent stem cells (iPSC-MNs). Using CRISPR-Cas9 technology and antisense oligonucleotides (ASOs), we found that the loss of EXOC2 activity suppresses disease-like phenotypes such as neuronal cell death and neurite degeneration, and, surprisingly, did so by reducing the levels of poly(GR) and expanded $G_4C_2$ repeats-containing RNA. Our findings indicate that EXOC2 directly or indirectly regulates the level of $G_4C_2$ repeats-containing RNA and may serve as a potential therapeutic target in *C9ORF72*-ALS/FTD.

## RESULTS

### *Sec5* is a genetic modifier of poly(GR) toxicity in *Drosophila* neurons

We previously identified *sec5* as a genetic suppressor of poly(GR) toxicity in non-neuronal *Drosophila* cells.[21] To examine whether partial knockdown of *sec5* suppresses poly(GR) toxicity in neuronal cells, we expressed poly(GR) in *Drosophila* photoreceptor neurons at the adult stage only. In this experiment, 80 copies of GR ($GR_{80}$) with a FLAG tag at the N terminus were expressed from the $(GGXCGX)_{80}$ sequence with an AUG start codon in photoreceptor neurons under the control of *GMR-Gal4* in the presence of the temperature-sensitive yeast transcription suppressor Gal80 ($Gal80^{ts}$).[21,31] At 1–3 days of age, adult male and female flies were shifted from 18°C to 25°C, a temperature at which Gal80 does not inhibit Gal4-mediated poly(GR) transcription anymore.[21,31] Control flies had a normal eye phenotype characterized by well-organized ommatidia and lack of necrosis (Figure S1A). $(GR)_{80}$ expression led to an eye degeneration phenotype characterized by disarrangements in ommatidia and necrosis (Figure S1A). Partial loss of *sec5* in two different RNAi lines suppressed poly(GR) toxicity in the eye (Figures S1A and S1B). The efficiency of *sec5* RNAi knockdown was confirmed by qRT-PCR (Figure S1C).

### Generation and characterization of *EXOC2* deletion in *C9ORF72* patient iPSCs

The human ortholog of *Drosophila Sec5, EXOC2*, encodes an essential subunit of the exocyst complex that plays a key role in multiple cellular processes.[28–30] To investigate whether and how EXOC2 regulates poly(GR) toxicity in human neurons, we first did western blot analyses of 3-week-old and 3-month-old iPSC-MNs and found no age-dependent change in EXOC2 levels between *C9ORF72* patient neurons and their isogenic controls lacking expanded $G_4C_2$ repeats[21] (Figures 1A and 1B).

Next, we used CRISPR-Cas9 technology[32,33] to mutate *EXOC2* in iPSC lines from two *C9ORF72*-ALS/FTD patients that caused a 97-nt deletion in exon 13 and intron 13 (Figure 1C). The deletion was confirmed by PCR analysis of genomic DNA (Figure S2A). Sanger sequencing analysis further confirmed the 97-nt deletion present in all cells that leads to a frameshift and a premature stop codon (Figure S2B). Indeed, qRT-PCR analysis showed a near-complete loss of *EXOC2* mRNA in iPSC-MNs with *EXOC2* homozygous deletion (*EXOC2*-del) (Figure 1D). Western blot analysis confirmed the complete loss of full-length EXOC2 protein (Figure 1E)–a surprising result because EXOC2 is required for cell viability.[34,35] However, a truncated EXOC2 fragment was detected at a low level in *EXOC2*-del iPSC-MNs differentiated from all three deletion iPSC lines, although the signal of the truncated band showed variability among the three lines (Figure 1E). The size of the truncated fragment corresponded to the fragment expected from the premature stop codon after CRISPR editing in *EXOC2*-del lines. Evidently, the EXOC2 fragment retains enough function to maintain cell viability. qRT-PCR analysis showed a 50% reduction in *EXOC2* mRNA in iPSC-MNs carrying the *EXOC2* heterozygous deletion (*EXOC2*-het del) (Figure S2C). However, the EXOC2 protein level in *EXOC2*-het del iPSC-MNs did not differ from that in the parental line (Figures S2D and S2E), indicating that a 50% reduction in *EXOC2* mRNA is not sufficient to decrease its protein level, probably because it exists in the exocyst complex. Therefore, only *EXOC2*-del lines (homozygous deletion) were used for the rest of the study. Karyotyping analysis confirmed the absence of chromosomal abnormalities in these CRISPR-edited iPSC lines (Figure S2F).

Next, we determined whether *EXOC2*-del lines show partial loss of EXOC2 function. Indeed, 3-week-old *EXOC2*-del iPSC-MNs had fewer primary dendrites than parental neurons (Figures 1F and 1G), consistent with a previous report.[34] Since exocyst helps localize *N*-methyl-D-aspartate receptors (NMDARs) to the plasma membrane,[36] we analyzed the surface localization of NMDARs. In neurons transduced with GFP-expressing lentivirus, the NMDAR 2B signal showed a significant reduction in surface localization in *EXOC2*-del neurons (Figures 1H and 1I), but the total level of NMDAR 2B appeared to be the same as that in parental neurons (Figures S2G and S2H). Thus, a change in total NMDAR 2B expression level was not responsible for the decrease in NMDARs on neuronal cell membranes. These results suggest that *EXOC2*-del lines exhibit a partial loss of EXOC2 function.

## *EXOC2* deletion rescues disease-relevant cellular phenotypes in *C9ORF72* iPSC-derived patient motor neurons

Expression of cleaved caspase 3 (CC3) level, an apoptosis induction marker, is greatly increased in 3- to 4-month-old *C9ORF72* iPSC-MNs.[21] To investigate whether *EXOC2* deletion rescues apoptotic cell death, we examined CC3 levels in 3-month-old isogenic control, *C9ORF72*, and *EXOC2*-del iPSC-MNs. The CC3 level was variably but significantly higher in *C9ORF72* iPSC-MNs than in isogenic controls (Figures 2A and 2B). In *C9ORF72* neurons from patient 1, *EXOC2* deletion decreased the CC3 level; in *EXOC2*-del *C9ORF72* neurons from patient 2, the level was even lower than in the isogenic controls (Figures 2A and 2B).

Cortical neurons derived from iPSCs of *C9ORF72* patients have more neurite degeneration than isogenic control neurons after 2–3 weeks of neurotrophic factor withdrawal.[31] To examine whether *EXOC2* deletion rescues neurite degeneration, we deprived iPSC-MNs of different genotypes of neurotrophic factor for 3 weeks. Neurite degeneration was significantly greater in *C9ORF72* iPSC-MNs than in isogenic controls and was also rescued in *EXOC2*-del iPSC-MNs in both patient lines (Figures 2C and 2D).

Dysregulation of autophagy is another feature of *C9ORF72*-ALS/FTD. In *C9ORF72* patient iPSC-derived neurons, levels of the selective autophagy receptor protein p62 are increased, and DPRs colocalize with p62 inclusions.[37,38] We found that the p62 level was significantly higher in 2-month-old *C9ORF72* iPSC-MNs than in isogenic controls; this phenotype was rescued in *EXOC2*-del iPSC-MNs differentiated from both patient lines (Figures 2E and 2F).

## *EXOC2* deletion reduces transcripts containing expanded $G_4C_2$ repeats in *C9ORF72* iPSC-MNs

To examine whether decreased DPR levels were responsible for the rescue of disease-relevant cellular phenotypes such as neuronal cell death and p62 accumulation, we measured poly(GR) levels with a Meso Scale Discovery immunoassay in a blinded manner.[21,31,39] The poly(GR) level was much lower in *EXOC2*-del iPSC-MNs than in *C9ORF72* iPSC-MNs differentiated from both patient lines (Figure 3A).

To further explore the mechanism by which *EXOC2* deletion reduces the poly(GR) level, because $G_4C_2$ repeat-containing RNA is the template for poly(GR) expression, we analyzed the levels of two variants, V1 and V3, which are splicing products of the expanded $G_4C_2$ repeat-containing *C9ORF72* pre-mRNA. We used primers specific to V1 and V3 mRNAs[31] (Figure 3B) and found that their levels in *C9ORF72* neurons were lower than that in isogenic control neurons (Figure S3A), consistent with our earlier result comparing *C9ORF72* neurons with non-isogenic control neurons.[37] We also found, surprisingly, that both V1 and V3 mRNA levels were significantly lower in *EXOC2*-del iPSC-MNs than *C9ORF72* iPSC-MNs differentiated from both patient lines (Figures 3C and 3D). To confirm this finding, we differentiated *C9ORF72* iPSC lines and EXOC2-del *C9ORF72* iPSC lines again and measured *EXOC2* mRNA (Figure S3B), V1 (Figure S3C), and V3 mRNA (Figure S3D) levels in a blinded manner and obtained the same result. We also quantified in a blinded manner the number of repeats-containing RNA foci (Figures S3E and S3F), the level of poly(GR) (Figure S3G), and the level of poly(GA) (Figure S3H) that is also translated from expanded $G_4C_2$ repeat RNA, and found they were all greatly reduced in *C9ORF72* MNs with *EXOC2* deletion. Next, we analyzed the allele-specific expression of *C9ORF72*-V3, taking advantage of the rs10757668 SNP (A/G) within exon 2.[4,31,40] While the wild-type allele is associated with nucleotide A, the mutant allele containing expanded $G_4C_2$ repeats is associated with nucleotide G (Figure 3E). The SNP G is present in patient 1 but not patient 2 neurons and preferentially expressed more than the A allele as shown by pyrosequencing and allele-specific quantification (Figure 3F). The relative level of the G allele was lower in *EXOC2*-del *C9ORF72* iPSC-MNs than in the parental *C9ORF72* iPSC-MNs of patient 1 (Figure 3F). To confirm this result, we used ASOs (see below) to knock down EXOC2

expression level in iPSC-derived MNs of another patient with the SNP G and confirmed the preferential downregulation of expanded $G_4C_2$ repeats-containing RNA (Figure S3I), albeit to a lesser extent. These findings suggest that *EXOC2*, either directly or indirectly, preferentially regulates the level of *C9ORF72* RNAs containing expanded $G_4C_2$ repeats.

## *EXOC2*-specific ASOs reduce levels of mRNA and pre-mRNA containing expanded $G_4C_2$ repeats in *C9ORF72* iPSC-MNs

Our finding that *EXOC2* deletion decreases the levels of *C9ORF72* transcripts containing expanded $G_4C_2$ repeats was surprising because EXOC2 has no known role in transcription or repeat RNA stability. It may do so indirectly through yet-to-be-identified molecular pathways. Moreover, it is unknown whether knocking down *EXOC2* in postmitotic mature *C9ORF72* patient neurons rescues disease phenotypes without affecting neuronal integrity. To address these questions, we used two ASOs to knock down *EXOC2* in iPSC-MNs of two *C9ORF72* patients and two healthy controls (Figure S4A). Control ASO did not change the *EXOC2* mRNA level, whereas *EXOC2* ASOs reduced the *EXOC2* mRNA level by 70%–80% (Figure S4B), and as a result, EXOC2 protein was decreased by 50%–60% (Figures S4C and S4D).

qRT-PCR analysis revealed a significant decrease in the *C9ORF72*-V1 mRNA level in ASO-treated motor neurons differentiated from iPSC lines of two *C9ORF72* patients (Figure S4E). qRT-PCR analysis of the *C9ORF72*-V3 mRNA level also showed similar results (Figure S4F). Using primers specific to the V1/V3 pre-mRNA (Figure 3B) also revealed a significant decrease in neurons of both patients (Figure S4G), indicating that the level of expanded $G_4C_2$ repeats-containing RNA is greatly down-regulated in *C9ORF72* neurons without EXOC2. However, in both patient and healthy control neurons, ASO treatment did not alter *C9ORF72*-V2 levels in transcripts encoding full-length *C9ORF72* protein lacking the $G_4C_2$ repeat sequence (Figure S4H).

## Treatment of *C9ORF72* iPSCs-derived mature motor neurons with *EXOC2* ASOs rescues disease phenotypes

Early loss of EXOC2 results in neurodevelopmental defects in animal models and patients.[34,35] In contrast, ALS and FTD are age-dependent neurodegenerative disorders that arise in mid- to late adulthood. Since the loss of EXOC2 also ameliorated disease phenotypes associated with *C9ORF72*-ALS/FTD, we investigated the potential therapeutic implications of *EXOC2* ASOs in iPSC-MNs. Old neurons tend to form large clumps, making ASO uptake inefficient and rendering it impossible to evaluate the effect of *EXOC2* ASOs on apoptosis in 3-month-old neurons. Therefore, we implemented an ASO treatment regimen combined with a stress condition to detect apoptosis at an earlier time point. CC3 levels increase 18–40 h after neurotrophic factor withdrawal in *SOD1* patient iPSC-MNs.[41] Since neuronal maturation takes about 2 weeks, we treated mature neurons with control or *EXOC2* ASOs for 10 days, starting on day 16, withdrew neurotrophic factors for 40 h, and then examined apoptosis in neurons or phosphorylated neurofilament heavy chain (pNfH) level in the culture medium (Figure 4A).

ASO treatment reduced the EXOC2 protein level by 50%–60% in both mature *C9ORF72* and isogenic control iPSC-MNs (Figures 4B and 4C), which led to a reduction in the levels of $G_4C_2$ repeats-containing pre-mRNA (Figure 4D), but it did not change the number of $MAP2^+$ primary dendrites (Figures S4J and S4K) or mean neurite length per neuron (Figure S4L). Thus, later interventions in mature neurons result in the partial loss of function of EXOC2 without causing neurite outgrowth defects.

Next, we assessed the induction of apoptosis 40 h after neurotrophic factor withdrawal. The CC3 level was increased in *C9ORF72* neurons compared with control neurons, and *EXOC2* ASOs rescued this phenotype. As a control, *EXOC2* ASO did not alter the CC3 levels in isogenic control iPSC-MNs (Figures 4E and 4F).

In the same samples, we also measured the release of pNfH into the culture medium by ELISA. pNfH is released as a result of axonal damage, and an elevated pNfH level in cerebrospinal fluid is considered a diagnostic and prognostic biomarker for ALS.[42,43] We found that the pNfH level in the medium was higher in control ASO-treated *C9ORF72* iPSC-MNs than in isogenic controls. *EXOC2* ASOs rescued this phenotype, but it did not change the pNfH level in the medium of isogenic control iPSC-MNs (Figure 4G).

Lastly, to further confirm these findings, we used ASOs to knock down *EXOC2* mRNA expression by 70%–80% in MNs differentiated from an additional two *C9ORF72* patients and found that the level of V1/V3 pre-mRNA was significantly decreased as well (Figures 4H and 4I). Correspondingly, the pNfH levels in the medium of MN cultures from these two *C9ORF72* patients but not from two healthy subjects were decreased after *EXOC2* ASO treatment (Figure 4J). Evidently, the treatment of mature neurons with *EXOC2* ASOs can rescue disease phenotypes and reduce expanded $G_4C_2$ repeats-containing RNA levels without causing morphological defects in mature neurons.

## DISCUSSION

In this study, we identified *Sec5/EXOC2* as another genetic modifier of poly(GR) toxicity in fly photoreceptor neurons and *C9ORF72*-ALS/FTD iPSC-derived motor neurons. EXOC2 is an exocyst subunit that contains an IPT/TIG (immunoglobulin-like fold, plexins, transcription factors/transcription factor immunoglobulin) domain, which is found in some receptors and several transcription factors (e.g., NF-kB and NFAT).[44–47] CRISPR-Cas9-mediated deletion of *EXOC2* in iPSCs or ASO-mediated partial knockdown of *EXOC2* in mature *C9ORF72* iPSC-MNs rescued disease-relevant cellular phenotypes such as apoptosis and neurite degeneration. Surprisingly, the loss of EXOC2 reduced toxic poly(GR) levels by directly or indirectly decreasing the level of RNAs containing expanded $G_4C_2$ repeats. Because of this unexpected result, we could not examine whether the loss of EXOC2 could also modulate poly(GR) toxicity itself in patient neurons in a way similar to that in flies. Nonetheless, our findings suggest that EXOC2 directly or indirectly affects the level of RNAs containing expanded $G_4C_2$ repeats through a to-be-identified pathway.

We generated CRISPR-Cas9-mediated homozygous deletion lines of *EXOC2* in *C9ORF72* iPSC-MNs that express a truncated N-terminal EXOC2 fragment at a low level.

Complete loss of EXOC2 and other exocyst subunits causes cell death and is embryonic lethal.[34,35,48,49] Our findings suggest that a truncated fragment of EXOC2 retains enough function to maintain cell viability. After we made this surprising observation, homozygous *EXOC2* deletion mutations were identified in patients with a neurodevelopmental disorder characterized by intellectual disability, developmental delay, and brain abnormalities.[35] As a remarkable coincidence, that study reported that two adult patients with a homozygous deletion mutation produce a truncated EXOC2 fragment similar in size to the one generated in our *C9ORF72* iPSC lines. Thus, a low level of the N-terminal EXOC2 fragment is sufficient to retain most of the function of the protein.

Using genetic knockout and ASO knockdown approaches, we found that the loss of EXOC2 function rescues neurodegeneration in *C9ORF72* patient neurons. Thus, *EXOC2* is another genetic modifier of the toxicity associated with expanded $G_4C_2$ repeats. Many genetic modifiers whose partial knockdown improves the neuronal survival of *C9ORF72*-ALS/FTD patient neurons have been reported, including the ones identified in our own lab such as *Ku80*,[21] *AFF2/FMR2*,[31] *p53*,[21] *HSP90*, and *TOPOII*.[50] It is not known whether variants in these genes influence the onset or progression of ALS/FTD. Our findings indicate that *EXOC2* knockdown by ASOs in mature *C9ORF72* patient neurons can rescue cellular phenotypes relevant to ALS/FTD without compromising neuronal morphology. Thus, *EXOC2* is a promising therapeutic target that merits further investigation.

### Limitations of the study

One limitation of the present study is that the molecular mechanism by which loss of EXOC2 decreases the level of expanded $G_4C_2$ repeats-containing RNA remains unknown. We were unable to obtain convincing evidence that EXOC2 somehow may directly regulate transcription of expanded $G_4C_2$ repeats in *C9ORF72*. Other potential mechanisms are also possible. For instance, EXOC2 is known to interact with upstream small GTPase RALB and then recruit TBK1 to activate downstream signaling and transcriptional events in innate immune responses.[51] Moreover, as part of the exocyst complex, EXOC2 regulates many other cellular processes.[29] It will be informative to examine how EXOC2 may act directly or indirectly through a specific molecular pathway to modulate the transcription and/or stability of expanded $G_4C_2$ repeats-containing RNA.

## STAR★METHODS

### RESOURCE AVAILABILITY

**Lead contact—**Further information and requests for resources and reagents should be directed to and will be fulfilled by the lead contact, Fen-Biao Gao (fen-biao.gao@umassmed.edu)

**Materials availability—**Requests for resources and additional information should be directed to and will be fulfilled by the lead contact. Reagents generated in this study will be made available on request, but we may require a completed Materials Transfer Agreement if there is potential for commercial application.

### Data and code availability

- Data supporting all the findings in this study are presented within the article and the supplementary information.
- This paper does not report original code.
- Any additional information required to reanalyze the results reported in this study is available from the lead contact upon request.

## EXPERIMENTAL MODEL AND STUDY PARTICIPANT DETAILS

**iPSC culture—**Two iPSC lines from *C9ORF72* carriers, 26L6 (Patient 1) and 27L11 (Patient 2), their isogenic control iPSC lines, 26Z90 (Control 1) and 27M91 (Control 2), three C9 patient iPSC lines, 16L14 (Patient 3), 40L3 (Patient 4) and 29iALS (Patient 5, for pyrosequencing), as well as iPSC lines from healthy subjects, 2L20 (Control 3) and 37L20 (Control 4) have been used before.[21,37] iPSCs were cultured as described.[21,50] Briefly, iPSCs were maintained in mTeSR1 medium (mTeSR1 Basal Medium with mTeSR1 5X supplement, Stem Cell Technologies) in six-well plates coated with Matrigel (cat. no. 354230, Corning), diluted 1:100 in KnockOut DMEM/F-12 (cat. no. 12660012, Gibco). The mTeSR1medium was replaced daily. iPSCs were passaged every 4–6 days. Cells were washed with Dulbecco's phosphate-buffered saline (DPBS), dissociated in Accutase (Cat no. SCR005, Millipore) diluted 1:2 in DPBS for ~1 min at room temperature (RT), washed with DPBS, and scraped in fresh mTeSR1 medium with a cell lifter. After reaching the desired colony size, cells were seeded n fresh mTeSR1 medium in Matrigel-coated six-well plates. Spontaneously differentiated colonies were manually removed, split, and differentiated into motor neuron.

**Motor neuron differentiation—**iPSCs were differentiated into spinal motor neurons as described.[21,52] At ~ 50% confluency, small colonies of iPSCs were seeded in mTeSR1 medium in Matrigel-coated six-well plates. Next day, the medium was replaced with neuroepithelial progenitor (NEP) induction medium consisting of neural medium KnockOut DMEM/F-12 medium (cat. no. 12660012, Gibco) and Neurobasal medium (cat. no 21103049, Gibco) (1:1), 0.5X N2 Supplement (cat. no. 17502-048, Gibco), 0.5X B27 Supplement (cat. no. 17504044, Gibco), 0.1 mM ascorbic acid (cat. no. A4403, Sigma), 1X Glutamax (cat. no. 35050061, Thermo Fisher Scientific), supplemented with 3 μM CHIR99021 (cat. no. 72054, Stem Cell Technologies), 2 μM DMH1 (cat. no. 4126, Tocris Bioscience), and 2 μM SB431542 (cat. no. 04-0010-10, Stemgent). NEP medium was changed every other day for 6 days. NEPs were dissociated with 1:2 diluted Accutase and split 1:3 into Matrigel-coated six-well plates. NEPs were cultured in motor neuron progenitor (MNP) induction medium, the neural medium supplemented with 1 μM CHIR99021, 2 μM DMH1, 2 μM SB431542, 0.1 μM retinoic acid (cat. no. R2625, Sigma), and 0.5 μM Purmorphamine (cat. no. 540220, Calbiochem). MNP medium was changed every other day for 6 days. MNPs were dissociated with 1:2 diluted Accutase and cultured in suspension in motor neuron differentiation medium, neural medium supplemented with 0.5 μM retinoic acid and 0.1 μM purmorphamine) in 60- mm low-attachment plates for 6 days. The media were changed every other day for 6 days. Lastly, neurospheres were dissociated into single cells with Accutase for 10 min at 37°C, passed through a 40 μm filter

into motor neuron medium. The neural medium supplemented with 0.5 μM retinoic acid, 0.1 μM purmorphamine, 0.1 μM Compound E (cat. no. 73954, Stem Cell Technologies), 10 ng/mL BDNF (cat. no. 248-BDB, R&D Systems), 10 ng/mL GDNF (cat. no. PHC7041, Thermo Fisher Scientific), and 1 μg/mL laminin (cat. no. L2020, Sigma). Cells were seeded in Matrigel-coated 12-well plates at $6x10^5$ cells/well density in motor neuron medium. For immunofluorescence staining experiments, cells were seeded onto poly-D-lysine/laminin-coated coverslips (cat. no. 354087, Corning) in 24-well plates in motor neuron medium at $3\text{-}6x10^4$ cells/well. After two weeks, neurons were maintained in motor neuron medium without retinoic acid or purmorphamine for up to 3 months; the medium was half-changed once a week for 3 weeks, and twice a week thereafter.

***Drosophila* strains and genetics—**Flies were maintained at 25°C on standard food. *UAS-(GR)$_{80}$* line was generated previously in our laboratory.[16] *UAS-GFP*, *w$^{1118}$* (BL3605), *GMR-Gal4* (BL9146), *Tub-Gal80$^{ts}$* (BL7019), *UAS-Sec5 RNAi*-1 (BL27526), *UAS-Sec5 RNAi*-2 (BL50556) lines were from the Bloomington *Drosophila* Stock Center.

## METHOD DETAILS

**Gene editing in iPSC lines—**CRISPR/Cas9 technology was used to create a deletion in *EXOC2* as described[32,33] with some modifications. Two sgRNAs targeting *EXOC2* were designed with CHOPCHOP in CRISPR/Cas9 knockout mode (https://chopchop.cbu.uib.no/, see Table S1). sgRNAs were cloned into pCAG-eCas9-GFP-U6-gRNA plasmid (Key Resources Table) and nucleofected into iPSCs. Cells with high GFP expression were FACS sorted and seeded at very low density (50,000 cells/plate) in Matrigel-coated 100-mm dishes. Single colonies were picked and seeded in Matrigel-coated 24-well plates and passaged for genotyping and maintenance. DNA was extracted with the DNeasy Blood & Tissue kit (cat. no. 69506, Qiagen) following the manufacturer's instructions. Colonies were screened by PCR (see primers in Table S1) and agarose gel electrophoresis. The deletions were confirmed in selected colonies by Sanger sequencing.

**RNA extraction and real-time quantitative PCR—**Total RNA from iPSC-MNs was extracted with the RNeasy Mini kit (cat. no. 74106, Qiagen). RNA (0.25–1 μg) was reverse transcribed to cDNA with random hexamers and the TaqMan Reverse Transcription kit (cat. no. N8080234, Thermo Fisher Scientific). Real-time quantitative PCR was done with SYBR Select Master Mix (cat. no. 4472918, Thermo Fisher Scientific) and an Applied Biosystems Quant Studio 3 System. Ct values for each sample were normalized to *cyclophilin*. Relative mRNA levels of each gene were calculated with the $2^{-\Delta\Delta Ct}$ method. (See Table S1 for the qRT-PCR primers).

**Pyrosequencing for *C9ORF72* allele specific expression—**Total RNA from *C9ORF72*-26 and *EXOC2* del iPSC-MNs was used to generate cDNA with OneStep RT-PCR Master Mix (cat. no. 978801, Qiagen) and previously described V3-specific primers.[31] Pyrosequencing for allele-specific quantification and data analysis were done by EpigenDx Inc. (Hopkinton, MA) in a blinded manner, using a previously described sequencing primer[31] (Table S1).

**Western blotting—**iPSC-MNs were washed with PBS and lysed in RIPA buffer (cat. no. 89901, Thermo Fisher Scientific) containing EDTA-free Halt Protease and Phosphatase Inhibitor Cocktail (100X) (cat. no. 78441, Thermo Fisher Scientific). Lysates were incubated on ice for 15 min, sonicated on ice at a 50% pulse rate for 10 s and centrifuged at 16,000 x *g* for 20 min at 4°C. The supernatant was collected, and protein concentration was determined with the Pierce BCA protein assay (cat. no. 23227, Thermo Fisher Scientific). Protein (20 μg) was mixed with 2X Laemmli Sample Buffer (cat. no. 1610737, Bio-Rad) containing β-mercaptoethanol (cat. no. M3148, Sigma) and boiled at 95°C for 10 min. Protein (60 μg) was loaded for detection of Cleaved caspase 3 and truncated fragments of EXOC2. Samples were run on SDS-PAGE gel, transferred to PVDF membranes, incubated with the primary antibodies listed in Key Resources Table at 4°C overnight. After washing three times with TBS-T, the membranes were incubated with secondary antibodies IRDye 680 goat anti-rabbit (cat. no. 926–68071, LI-COR Biosciences) and/or IRDye 800CW donkey anti-mouse (cat. no. 926–32212, LI-COR Biosciences) for 1 h at room temperature (RT). Odyssey Blocking Buffer (cat. no. 927–40010, LI-COR Biosciences) was used for blocking and antibody dilutions. The images were acquired with the Odyssey Imaging System (LI-COR Biosciences).

**Dot blot—**iPSC-MN lysates were prepared as described above. Duplicate samples (20 μg protein) were loaded onto the Bio-Dot Microfiltration System dot blot module (cat. no. 1703938, Bio-Rad) transferred to a nitrocellulose membrane in vacuum mode following manufacturer's instructions and stained with Ponceau S for detection of total protein. Samples were incubated with primary and secondary antibodies as described for western blotting.

**Immunofluorescence staining—**iPSC-MNs were fixed in 4% paraformaldehyde for 10 min at RT and permeabilized with 0.2% Triton X-100 for 5 min (except for surface NMDAR staining experiments), blocked with 3% BSA for 30 min at RT, and incubated with primary antibodies (Key Resources Table) for 1 h at RT. After three washes with PBS, cells were incubated with donkey anti-mouse IgG Alexa Fluor 488 (cat. no. A-21202, Thermo Fisher Scientific) and/or Donkey anti-Rabbit IgG Alexa Fluor 568 (cat. no. A-10042, Thermo Fisher Scientific; 1:500) for 1 h at RT. Coverslips were mounted with Prolong Glass Antifade Mountant with NucBlue Stain (cat. no. P36981, Thermo Fisher Scientific). Images were acquired with Zeiss LSM 800 microscope equipped with an AxioCam 506 camera.

**Karyotyping analysis—**Two 25cm flasks (50% confluent) per iPSC line were shipped to KaryoLogic Inc. (Durham, NC). 10% FBS was added to the media to reduce detachment.

**Lentivirus production—**Lentiviral eGFP expression vector was purchased from Addgene (Plasmid#17448) and GFP-expressing lentivirus was generated in HEK cells as described.[54]

**ASO treatment in iPSC-MNs—**Control ASO (nontargeting control) and two *EXOC2* ASOs were designed by and purchased from IDT Custom Design Service. The ASOs were 20 nt long and contained the following modifications: phosphorothioate linkage in backbone, 5-10-5 gapmer structure with 2′-*O*-methoxy-ethyl bases (2′-MOE). ASOs (5 or 10 μM) were directly added to culture medium for treatment of iPSC-MNs.

**MSD assay—**Poly(GR) from iPSC-MNs was measured with an MSD immunoassay as described.[31,39] iPSC-MN lysates were prepared in RIPA buffer as described in Western blotting Section. Samples were adjusted to an amount of 50 μg/well with Tris-buffered saline (TBS) and tested in duplicate wells on 96-well plate (cat. no. L45XA, MSD) precoated with a custom-made polyclonal rabbit anti-$(GR)_8$ antibody (1 μg/mL; Covance). Anti-$(GR)_8$ antibody tagged with GOLD SULFO (0.5 μg/mL; cat. no. R31AA, Meso SCale Discovery) was used as detection antibody. Signals were detected using QuickPlex SQ120 Instrument (Meso Scale Discovery). For background correction, values from samples were subtracted those of corresponding isogenic control iPSC-MNs. Similarly, poly(GA) was quantified as reported before.[39]

**Detection of phosphorylated neurofilament heavy chain (pNFH)—**Culture medium from iPSC-MNs was collected 40 h after withdrawal of neurotrophic factor. Samples were briefly centrifuged to remove debris and supplemented with protease and phosphatase inhibitor. The pNFH signal was measured in medium diluted 1:2.5 with the pNFH ELISA kit (cat. no. ELISA-pNF-H-V2, EnCor Biotechnology) following the manufacturer's instructions.

## QUANTIFICATION AND STATISTICAL ANALYSIS

**Neurite degeneration index—**iPSC-MNs stained with Tuj1 antibody were imaged with a 20x objective as described above. The ratio of degenerated neurites to total area (degeneration index) was calculated as described.[31,53] Briefly, images were binarized and the particle analyzer of ImageJ was used to quantify 20–10,000 pixels or degenerated neurites and 20–infinity pixels for total area.

**Neurite quantification—**iPSC-MNs stained for MAP2 were imaged with a 20x objective as described above. Neurites were traced with the NeuronJ plugin in ImageJ to quantify the number of primary dendrites (defined as those originating from the soma). Average neurite length per neuron was also quantified using NeuronJ, limiting measurement to primary dendrites from soma to the first branchpoint.

**Quantification of *Drosophila* external eye phenotype—**The external eye phenotype of control and $(GR)_{80}$-expressing flies was characterized as described.[50] Briefly, flies were raised at 23°C for 14 days. Adult flies were immobilized and examined under a dissecting microscope. The phenotype was categorized as absent, weak, or medium based on ommatidia structure, pigmentation, and level of necrosis.

**Statistical analysis—**Values are reported as mean ± S.E.M. GraphPad Prism software (version 9.5.1) was used for statistical analysis. Unpaired two-tailed *t*-tests were used to compare two groups. One-way ANOVA with Dunnett's or Tukey's multiple comparisons tests were used to compare three or more groups.

## Supplementary Material

Refer to Web version on PubMed Central for supplementary material.

## ACKNOWLEDGMENTS

We thank the Bloomington *Drosophila* Stock Center for fly lines, and University of Massachusetts Chan Medical School Flow Cytometry Core for fluorescence-activated cell sorting iPSCs. D.O.H. thanks her thesis research advisory committee members David Weaver, Mary Munson, Eric Baehrecke, and Hong Zhang, as well as external examiner Rita Sattler for guidance. This work was supported by NIH grants R37NS057553 and R01NS101986 (to F.-B.G.) and R01HD104971 (to T.G.F.). S.A. is funded by NIH grants R21NS119952 and R21NS112766. The antibodies used to measure GA levels were discovered by Neurimmune AG (Zurich, Switzerland).

## REFERENCES

1. Ling SC, Polymenidou M, and Cleveland DW (2013). Converging mechanisms in ALS and FTD: disrupted RNA and protein homeostasis. Neuron 79, 416–438. 10.1016/j.neuron.2013.07.033.
2. Gitler AD, and Tsuiji H (2016). There has been an awakening: Emerging mechanisms of C9orf72 mutations in FTD/ALS. Brain Res. 1647, 19–29. 10.1016/j.brainres.2016.04.004.
3. Gao FB, Almeida S, and Lopez-Gonzalez R (2017). Dysregulated molecular pathways in amyotrophic lateral sclerosis-frontotemporal dementia spectrum disorder. EMBO J. 36, 2931–2950. 10.15252/embj.201797568.
4. DeJesus-Hernandez M, Mackenzie IR, Boeve BF, Boxer AL, Baker M, Rutherford NJ, Nicholson AM, Finch NA, Flynn H, Adamson J, et al. (2011). Expanded GGGGCC hexanucleotide repeat in noncoding region of C9ORF72 causes chromosome 9p-linked FTD and ALS. Neuron 72, 245–256. 10.1016/j.neuron.2011.09.011.
5. Renton AE, Majounie E, Waite A, Simón-Sánchez J, Rollinson S, Gibbs JR, Schymick JC, Laaksovirta H, van Swieten JC, Myllykangas L, et al. (2011).A hexanucleotide repeat expansion in C9ORF72 is the cause of chromosome 9p21-linked ALS-FTD. Neuron 72, 257–268. 10.1016/j.neuron.2011.09.010.
6. Mori K, Weng SM, Arzberger T, May S, Rentzsch K, Kremmer E, Schmid B, Kretzschmar HA, Cruts M, Van Broeckhoven C, et al. (2013). The C9orf72 GGGGCC repeat is translated into aggregating dipeptide-repeat proteins in FTLD/ALS. Science 339, 1335–1338. 10.1126/science.1232927.
7. Ash PEA, Bieniek KF, Gendron TF, Caulfield T, Lin WL, Dejesus-Hernandez M, van Blitterswijk MM, Jansen-West K, Paul JW, Rademakers R, et al. (2013). Unconventional translation of C9ORF72 GGGGCC expansion generates insoluble polypeptides specific to c9FTD/ALS. Neuron 77, 639–646. 10.1016/j.neuron.2013.02.004.
8. Zu T, Liu Y, Bañez-Coronel M, Reid T, Pletnikova O, Lewis J, Miller TM, Harms MB, Falchook AE, Subramony SH, et al. (2013). RAN proteins and RNA foci from antisense transcripts in C9ORF72 ALS and frontotemporal dementia. Proc. Natl. Acad. Sci. USA 110, 4968–4977. 10.1073/pnas.1315438110.
9. Saberi S, Stauffer JE, Jiang J, Garcia SD, Taylor AE, Schulte D, Ohkubo T, Schloffman CL, Maldonado M, Baughn M, et al. (2018). Sense-encoded poly-GR dipeptide repeat proteins correlate to neurodegeneration and uniquely co-localize with TDP-43 in dendrites of repeat-expanded C9orf72 amyotrophic lateral sclerosis. Acta Neuropathol. 135, 459–474. 10.1007/s00401-017-1793-8.
10. Sakae N, Bieniek KF, Zhang YJ, Ross K, Gendron TF, Murray ME, Rademakers R, Petrucelli L, and Dickson DW (2018). Poly-GR dipeptide repeat polymers correlate with neurodegeneration and Clinicopathological subtypes in C9ORF72-related brain disease. Acta Neuropathol. Commun 6, 63. 10.1186/s40478-018-0564-7.
11. Quaegebeur A, Glaria I, Lashley T, and Isaacs AM (2020). Soluble and insoluble dipeptide repeat protein measurements in C9orf72-fronto-temporal dementia brains show regional differential solubility and correlation of poly-GR with clinical severity. Acta Neuropathol. Commun 8, 184. 10.1186/s40478-020-01036-y.
12. Kwon I, Xiang S, Kato M, Wu L, Theodoropoulos P, Wang T, Kim J, Yun J, Xie Y, and McKnight SL (2014). Poly-dipeptides encoded by the C9orf72 repeats bind nucleoli, impede RNA biogenesis, and kill cells. Science 345, 1139–1145. 10.1126/science.1254917.

13. Mizielinska S, Lashley T, Norona FE, Clayton EL, Ridler CE, Fratta P, and Isaacs AM (2013). C9orf72 frontotemporal lobar degeneration is characterised by frequent neuronal sense and antisense RNA foci. Acta Neuropathol. 126, 845–857. 10.1007/s00401-013-1200-z.

14. Wen X, Tan W, Westergard T, Krishnamurthy K, Markandaiah SS, Shi Y, Lin S, Shneider NA, Monaghan J, Pandey UB, et al. (2014). Antisense proline-arginine RAN dipeptides linked to C9ORF72-ALS/FTD form toxic nuclear aggregates that initiate in vitro and in vivo neuronal death. Neuron 84, 1213–1225. 10.1016/j.neuron.2014.12.010.

15. Jovičić A, Mertens J, Boeynaems S, Bogaert E, Chai N, Yamada SB, Paul JW 3rd, Sun S, Herdy JR, Bieri G, et al. (2015). Modifiers of C9orf72 dipeptide repeat toxicity connect nucleocytoplasmic transport defects to FTD/ALS. Nat. Neurosci 18, 1226–1229. 10.1038/nn.4085.

16. Yang D, Abdallah A, Li Z, Lu Y, Almeida S, and Gao FB (2015). FTD/ALS-associated poly(GR) protein impairs the Notch pathway and is recruited by poly(GA) into cytoplasmic inclusions. Acta Neuropathol. 130, 525–535. 10.1007/s00401-015-1448-6.

17. Lopez-Gonzalez R, Lu Y, Gendron TF, Karydas A, Tran H, Yang D, Petrucelli L, Miller BL, Almeida S, and Gao FB (2016). Poly(GR) in C9ORF72-related ALS/FTD compromises mitochondrial function and increases oxidative stress and DNA damage in iPSC-derived motor neurons. Neuron 92, 383–391. 10.1016/j.neuron.2016.09.015.

18. Zhang YJ, Gendron TF, Ebbert MTW, O'Raw AD, Yue M, Jansen-West K, Zhang X, Prudencio M, Chew J, Cook CN, et al. (2018). Poly(GR) impairs protein translation and stress granule dynamics in C9orf72-associated frontotemporal dementia and amyotrophic lateral sclerosis. Nat. Med 24, 1136–1142. 10.1038/s41591-018-0071-1.

19. Choi SY, Lopez-Gonzalez R, Krishnan G, Phillips HL, Li AN, Seeley WW, Yao WD, Almeida S, and Gao FB (2019). C9ORF72-ALS/FTD-associated poly(GR) binds Atp5a1 and compromises mitochondrial function in vivo. Nat. Neurosci 22, 851–862. 10.1038/s41593-019-0397-0.

20. Lee KH, Zhang P, Kim HJ, Mitrea DM, Sarkar M, Freibaum BD, Cika J, Coughlin M, Messing J, Molliex A, et al. (2016). C9orf72 dipeptide repeats impair the assembly, dynamics, and function of membraneless organelles. Cell 167, 774–788.e17. 10.1016/j.cell.2016.10.002.

21. Lopez-Gonzalez R, Yang D, Pribadi M, Kim TS, Krishnan G, Choi SY, Lee S, Coppola G, and Gao FB (2019). Partial inhibition of the overactivated Ku80-dependent DNA repair pathway rescues neurodegeneration in C9ORF72-ALS/FTD. Proc. Natl. Acad. Sci. USA 116, 9628–9633. 10.1073/pnas.1901313116.

22. Lin Y, Mori E, Kato M, Xiang S, Wu L, Kwon I, and McKnight SL (2016). Toxic PR poly-dipeptides encoded by the C9orf72 repeat expansion target LC domain polymers. Cell 167, 789–802.e12. 10.1016/j.cell.2016.10.003.

23. Boeynaems S, Bogaert E, Michiels E, Gijselinck I, Sieben A, Jovičić A, De Baets G, Scheveneels W, Steyaert J, Cuijt I, et al. (2016). Drosophila screen connects nuclear transport genes to DPR pathology in c9ALS/FTD. Sci. Rep 6, 20877. 10.1038/srep20877.

24. Yin S, Lopez-Gonzalez R, Kunz RC, Gangopadhyay J, Borufka C, Gygi SP, Gao FB, and Reed R (2017). Evidence that C9ORF72 dipeptide repeat proteins associate with U2 snRNP to cause mis-splicing in ALS/FTD patients. Cell Rep. 19, 2244–2256. 10.1016/j.celrep.2017.05.056.

25. Hartmann H, Hornburg D, Czuppa M, Bader J, Michaelsen M, Farny D, Arzberger T, Mann M, Meissner F, and Edbauer D (2018). Proteomics and C9orf72 neuropathology identify ribosomes as poly-GR/PR interactors driving toxicity. Life Sci. Alliance 1, e201800070. 10.26508/lsa.201800070.

26. Moens TG, Mizielinska S, Niccoli T, Mitchell JS, Thoeng A, Ridler CE, Grönke S, Esser J, Heslegrave A, Zetterberg H, et al. (2018). Sense and antisense RNA are not toxic in Drosophila models of C9orf72-associated ALS/FTD. Acta Neuropathol. 135, 445–457. 10.1007/s00401-017-1798-3.

27. Loveland AB, Svidritskiy E, Susorov D, Lee S, Park A, Zvornicanin S, Demo G, Gao FB, and Korostelev AA (2022). Ribosome inhibition by C9ORF72-ALS/FTD-associated poly-PR and poly-GR proteins revealed by cryo-EM. Nat. Commun 13, 2776. 10.1038/s41467-022-30418-0.

28. Heider MR, and Munson M (2012). Exorcising the exocyst complex. Traffic 13, 898–907. 10.1111/j.1600-0854.2012.01353.x.

29. Wu B, and Guo W (2015). The exocyst at a glance. J. Cell Sci 128, 2957–2964. 10.1242/jcs.156398.
30. Halim DO, Munson M, and Gao FB (2023). The exocyst complex in neurological disorders. Hum. Genet 142, 1263–1270. 10.1007/s00439-023-02558-w.
31. Yuva-Aydemir Y, Almeida S, Krishnan G, Gendron TF, and Gao FB (2019). Transcription elongation factor AFF2/FMR2 regulates expression of expanded GGGGCC repeat-containing C9ORF72 allele in ALS/FTD. Nat. Commun 10, 5466. 10.1038/s41467-019-13477-8.
32. Trevino AE, and Zhang F (2014). Genome editing using cas9 nickases. Methods Enzymol. 546, 161–174. 10.1016/B978-0-12-801185-0.00008-8.
33. Yang L, Yang JL, Byrne S, Pan J, and Church GM (2014). CRISPR/Cas9-directed genome editing of cultured cells. Curr. Protoc. Mol. Biol 107, 31.1.1–31.1.17. 10.1002/0471142727.mb3101s107.
34. Murthy M, Garza D, Scheller RH, and Schwarz TL (2003). Mutations in the exocyst component Sec5 disrupt neuronal membrane traffic, but neurotransmitter release persists. Neuron 37, 433–447. 10.1016/s0896-6273(03)00031-x.
35. Van Bergen NJ, Ahmed SM, Collins F, Cowley M, Vetro A, Dale RC, Hock DH, de Caestecker C, Menezes M, Massey S, et al. (2020). Mutations in the exocyst component EXOC2 cause severe defects in human brain development. J. Exp. Med 217, e20192040. 10.1084/jem.20192040.
36. Sans N, Prybylowski K, Petralia RS, Chang K, Wang YX, Racca C, Vicini S, and Wenthold RJ (2003). NMDA receptor trafficking through an interaction between PDZ proteins and the exocyst complex. Nat. Cell Biol 5, 520–530. 10.1038/ncb990.
37. Almeida S, Gascon E, Tran H, Chou HJ, Gendron TF, Degroot S, Tapper AR, Sellier C, Charlet-Berguerand N, Karydas A, et al. (2013). Modeling key pathological features of frontotemporal dementia with C9ORF72 repeat expansion in iPSC-derived human neurons. Acta Neuropathol. 126, 385–399. 10.1007/s00401-013-1149-y.
38. Mann DMA, Rollinson S, Robinson A, Bennion Callister J, Thompson JC, Snowden JS, Gendron T, Petrucelli L, Masuda-Suzukake M, Hasegawa M, et al. (2013). Dipeptide repeat proteins are present in the p62 positive inclusions in patients with frontotemporal lobar degeneration and motor neurone disease associated with expansions in C9ORF72. Acta Neuropathol. Commun 1, 68. 10.1186/2051-5960-1-68.
39. Krishnan G, Raitcheva D, Bartlett D, Prudencio M, McKenna-Yasek DM, Douthwright C, Oskarsson BE, Ladha S, King OD, Barmada SJ, et al. (2022). Poly(GR) and poly(GA) in cerebrospinal fluid as potential biomarkers for C9ORF72-ALS/FTD. Nat. Commun 13, 2799. 10.1038/s41467-022-30387-4.
40. Sareen D, O'Rourke JG, Meera P, Muhammad AKMG, Grant S, Simpkinson M, Bell S, Carmona S, Ornelas L, Sahabian A, et al. (2013). Targeting RNA foci in iPSC-derived motor neurons from ALS patients with a C9ORF72 repeat expansion. Sci. Transl. Med 5, 208ra149. 10.1126/scitranslmed.3007529.
41. Wu C, Watts ME, and Rubin LL (2019). MAP4K4 activation mediates motor neuron degeneration in amyotrophic lateral sclerosis. Cell Rep. 26, 1143–1156.e5. 10.1016/j.celrep.2019.01.019.
42. Verber NS, Shepheard SR, Sassani M, McDonough HE, Moore SA, Alix JJP, Wilkinson ID, Jenkins TM, and Shaw PJ (2019). Biomarkers in Motor Neuron Disease:A State of the Art Review. Front. Neurol 10, 291. 10.3389/fneur.2019.00291.
43. Witzel S, Mayer K, and Oeckl P (2022). Biomarkers for amyotrophic lateral sclerosis. Curr. Opin. Neurol 35, 699–704. 10.1097/WCO.0000000000001094.
44. Mott HR, Nietlispach D, Hopkins LJ, Mirey G, Camonis JH, and Owen D (2003). Structure of the GTPase-binding domain of Sec5 and elucidation of its Ral binding site. J. Biol. Chem 278, 17053–17059. 10.1074/jbc.M300155200.
45. Bork P, Doerks T, Springer TA, and Snel B (1999). Domains in plexins: links to integrins and transcription factors. Trends Biochem. Sci 24, 261–263. 10.1016/s0968-0004(99)01416-4.
46. Ghosh G, van Duyne G, Ghosh S, and Sigler PB (1995). Structure of NF-kappa B p50 homodimer bound to a kappa B site. Nature 373, 303–310. 10.1038/373303a0.
47. Duan X, Lv M, Liu A, Pang Y, Li Q, Su P, and Gou M (2021). Identification and evolution of transcription factors RHR gene family (NFAT and RBPJ) involving lamprey (Lethenteron reissneri) innate immunity. Mol. Immunol 138, 38–47. 10.1016/j.molimm.2021.07.017.

48. Friedrich GA, Hildebrand JD, and Soriano P (1997). The secretory protein sec8 Is required for paraxial mesoderm formation in the mouse. Dev. Biol 192, 364–374. 10.1006/dbio.1997.8727.

49. Mizuno S, Takami K, Daitoku Y, Tanimoto Y, Dinh TTH, Mizuno-Iijima S, Hasegawa Y, Takahashi S, Sugiyama F, and Yagami KI (2015). Peri-implantation lethality in mice carrying megabasescale deletion on 5qc3.3 is caused by Exoc1 null mutation. Sci. Rep 5, 13632. 10.1038/srep13632.

50. Lee S, Jun YW, Linares GR, Butler B, Yuva-Adyemir Y, Moore J, Krishnan G, Ruiz-Juarez B, Santana M, Pons M, et al. (2023). Downregulation of Hsp90 and the antimicrobial peptide Mtk suppresses poly(GR)-induced neurotoxicity in C9ORF72-ALS/FTD. Neuron 111, 1381–1390.e6. 10.1016/j.neuron.2023.02.029.

51. Chien Y, and White MA (2008). Characterization of RalB-Sec5-TBK1 function in human oncogenesis. Methods Enzymol. 438, 321–329.

52. Du ZW, Chen H, Liu H, Lu J, Qian K, Huang CL, Zhong X, Fan F, and Zhang SC (2015). Generation and expansion of highly pure motor neuron progenitors from human pluripotent stem cells. Nat. Commun 6, 6626. 10.1038/ncomms7626.

53. Sasaki Y, Vohra BPS, Lund FE, and Milbrandt J (2009). Nicotinamide mononucleotide adenylyl transferase-mediated axonal protection requires enzymatic activity but not increased levels of neuronal nicotinamide adenine dinucleotide. J. Neurosci 29, 5525–5535. 10.1523/JNEUROSCI.5469-08.2009.

54. Tiscornia G, Singer O, and Verma IM (2006). Production and purification of lentiviral vectors. Nat. Protoc 1, 241–245. 10.1038/nprot.2006.37.

55. Zhang Z, Almeida S, Lu Y, Nishimura AL, Peng L, Sun D, Wu B, Karydas AM, Tartaglia MC, Fong JC, et al. (2013). Downregulation of microRNA-9 in iPSC-derived neurons of FTD/ALS patients with TDP-43 mutations. PLoS One 8, e76055. 10.1371/joumal.pone.0076055.

56. Freibaum BD, Lu Y, Lopez-Gonzalez R, Kim NC, Almeida S, Lee KH, Badders N, Valentine M, Miller BL, Wong PC, et al. (2015). GGGGCC repeat expansion in C9orf72 compromises nucleocytoplasmic transport. Nature 525, 129–133. 10.1038/nature14974.

57. Stewart SA, Dykxhoorn DM, Palliser D, Mizuno H, Yu EY, An DS, Sabatini DM, Chen ISY, Hahn WC, Sharp PA, et al. (2003). Lentivirus-delivered stable gene silencing by RNAi in primary cells. RNA 9, 493–501. 10.1261/rna.2192803.

58. Campeau E, Ruhl VE, Rodier F, Smith CL, Rahmberg BL, Fuss JO, Campisi J, Yaswen P, Cooper PK, and Kaufman PD (2009). A versatile viral system for expression and depletion of proteins in mammalian cells. PLoS One 4, e6529. 10.1371/journal.pone.0006529.

## Highlights

- The N-terminal fragment of EXOC2 is sufficient to maintain cell viability
- Deletion of *EXOC2* in *C9ORF72*-ALS/FTD motor neurons rescues disease phenotypes
- *EXOC2* ASOs reduce axon degeneration and apoptosis in *C9ORF72* motor neurons
- Loss of EXOC2 decreases the levels of DPR proteins and expanded $G_4C_2$ repeats RNA

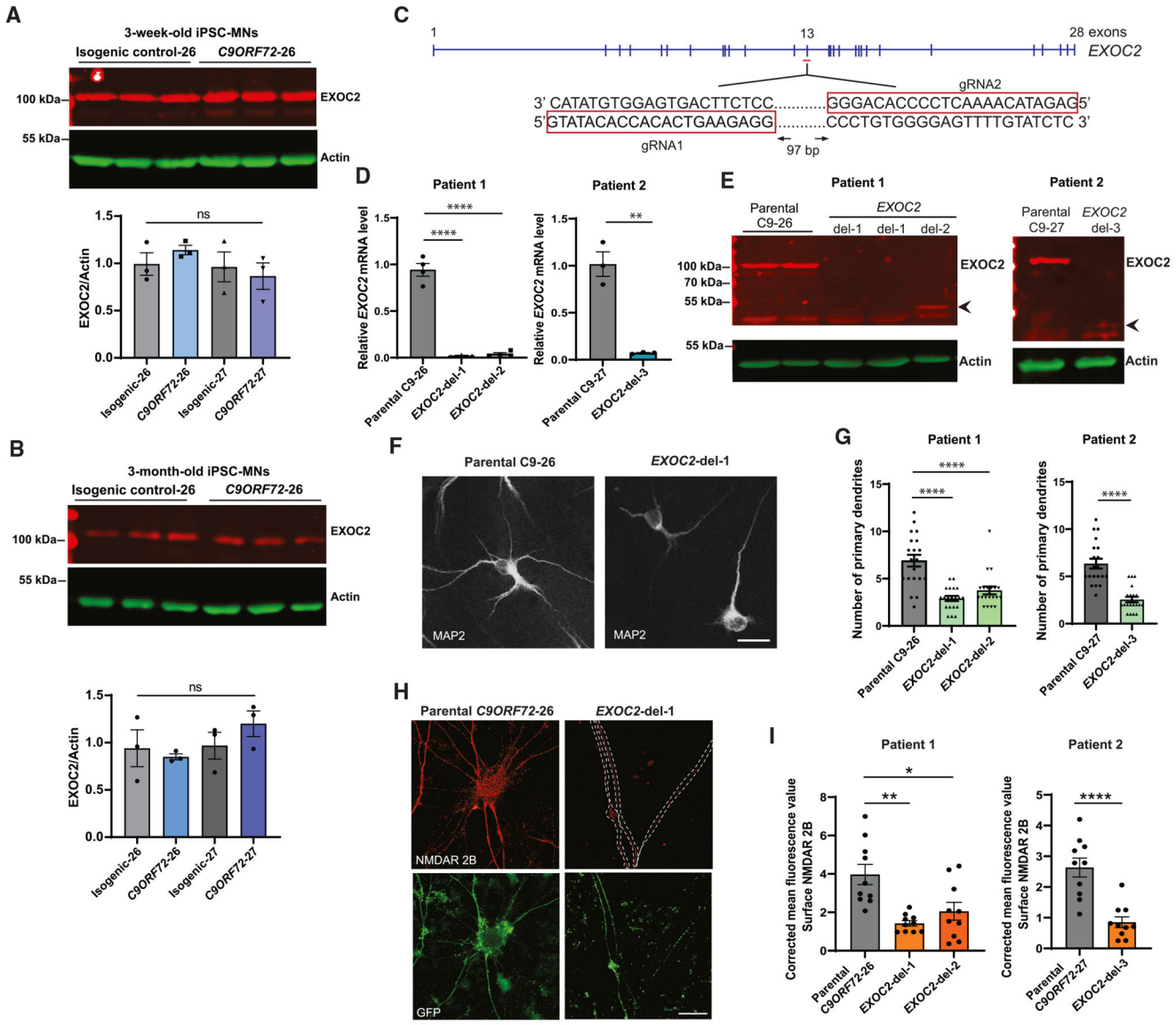


**Figure 1. Generation of a deletion in *EXOC2* by the CRISPR-Cas9 technology in iPSC lines derived from two *C9ORF72* patients**

(A and B) Representative western blot images of EXOC2 in 3-week-old (A) and 3-month-old (B) isogenic control and *C9ORF72* iPSC-MNs and densitometric quantification of EXOC2 protein level. Each data point represents one differentiation ($n = 3$ independent differentiations). Values are mean ± SEM. ns, not significant (one-way ANOVA with Tukey's multiple comparisons test).

(C) Schematic representation of the deletion in *EXOC2* near exon 13 in *C9ORF72* iPSC lines.

(D) qRT-PCR analysis of *EXOC2* mRNA levels in 3-week-old MNs differentiated from parental and *EXOC2* deletion iPSC lines (*EXOC2*-del iPSC-MNs).

(E) Representative western blot analysis of 3-week-old parental and *EXOC2*-del iPSC-MNs. Both samples in parental C9-26 or Del-1 came from the same iPSC line. Arrowhead indicates a truncated form of EXOC2, which is present but weaker in Del-1 lanes.
(F) Representative immunostaining images for the dendrite-specific marker MAP2 in 3-week-old parental and *EXOC2*-del iPSC-MNs.
(G) Quantification of the numbers of primary dendrites from *C9ORF72* and *EXOC2*-del iPSC-MNs as illustrated in (F). Twenty randomly chosen fields were quantified for analysis.
(H) Representative immunofluorescence image of surface NMDAR 2B staining in 3-week-old parental and *EXOC2*-del *C9ORF72* iPSC-MNs.
(I) Mean fluorescence values of NMDAR 2B from *C9ORF72* and *EXOC2*-del iPSC-MNs as illustrated in (H). Ten randomly chosen fields were quantified for analysis. Neurons were transduced with lentivirus expressing GFP. Each data point represents one differentiation in (D) and one neuron in (G) ($n$ = 3–4 independent differentiations). Values are mean ± SEM. $^{**}p < 0.01$; $^{****}p < 0.0001$ by one-way ANOVA with Dunnett's multiple comparisons (patient 1) and two-tailed Student's t test (patient 2). Scale bar, 20 μm.
See also Figures S1 and S2.

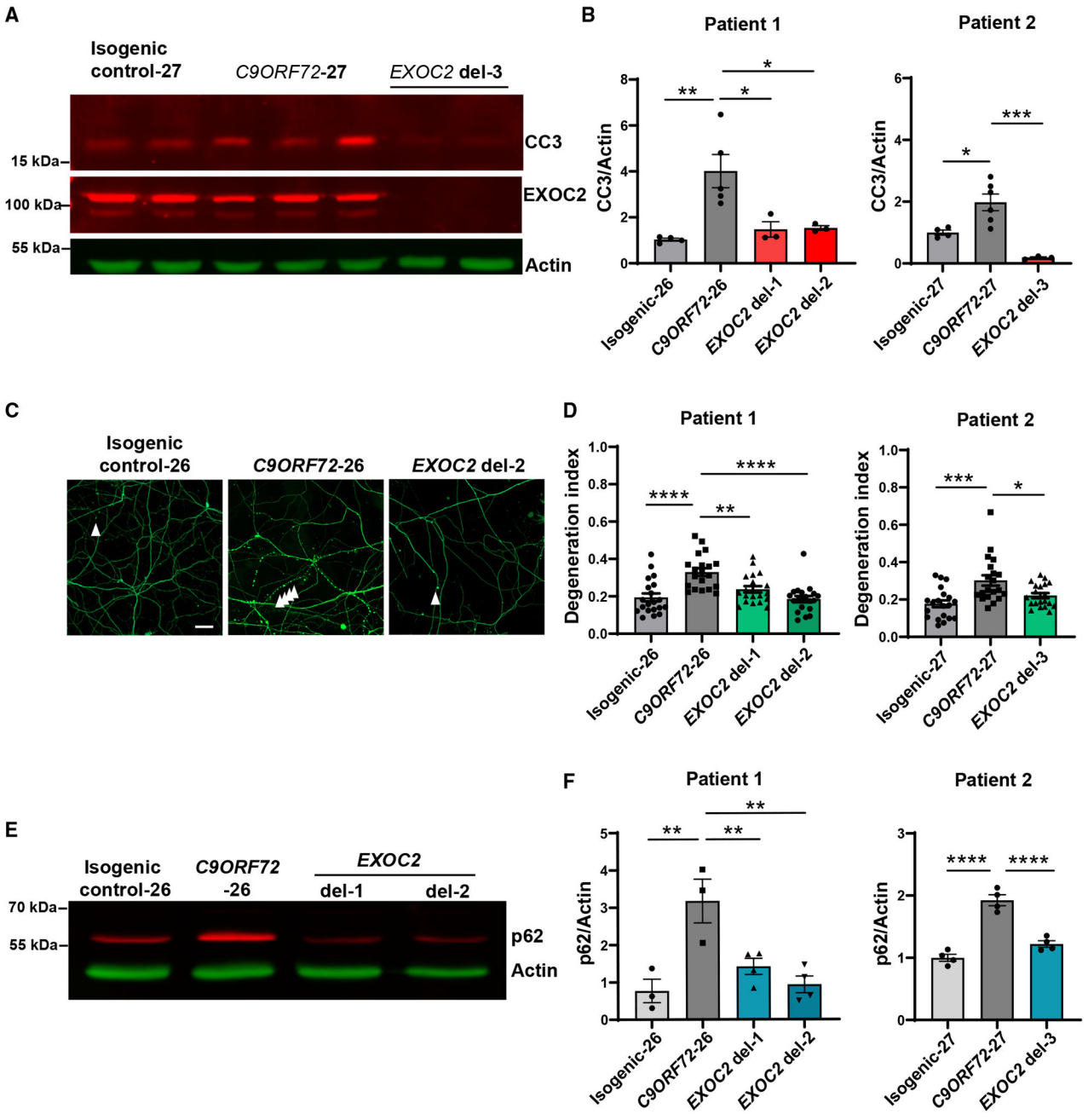


**Figure 2. *EXOC2* deletion rescues *C9ORF72*-ALS/FTD-related disease phenotypes**

(A and B) Representative images (A) and densitometric quantification (B) for western blot analysis of CC3 in 3-month-old isogenic control, *C9ORF72*, and *EXOC2*-del iPSC-MNs. The upper half of the blot was probed for EXOC2 and actin, and the lower half of the blot was probed for CC3.

(C) Representative images for immunostaining for TUJ1 showing neurite degeneration in 3-week-old isogenic control, *C9ORF72*, and *EXOC2*-del iPSC-MNs after neurotrophic factor withdrawal. Arrowheads indicate beading or fragmentation. Scale bar, 20 μm.

(D) Quantification of images as shown in (C) for MN cultures obtained from the two *C9ORF72* patients. Degeneration index was measured by the ratio of fragmented neurites over total area. Twenty randomly chosen fields were quantified for analysis.
(E) Representative images for western blot analysis of p62 level in 2-month-old isogenic control, *C9ORF72*, and *EXOC2*-del iPSC-MNs.
(F) Densitometric quantification of p62 protein level in 2-month-old cultures from isogenic control, *C9ORF72*, and *EXOC2*-del iPSC-MNs as shown in (E). Each data point in (B) and (F) represents one differentiation ($n$ = 3–6 independent differentiations); each data point in (D) represents one field. Values are mean ± SEM. *$p < 0.05$; **$p < 0.01$; ***$p < 0.001$; ****$p < 0.0001$ by one-way ANOVA with Dunnett's multiple comparisons test.
See also Figure S2.

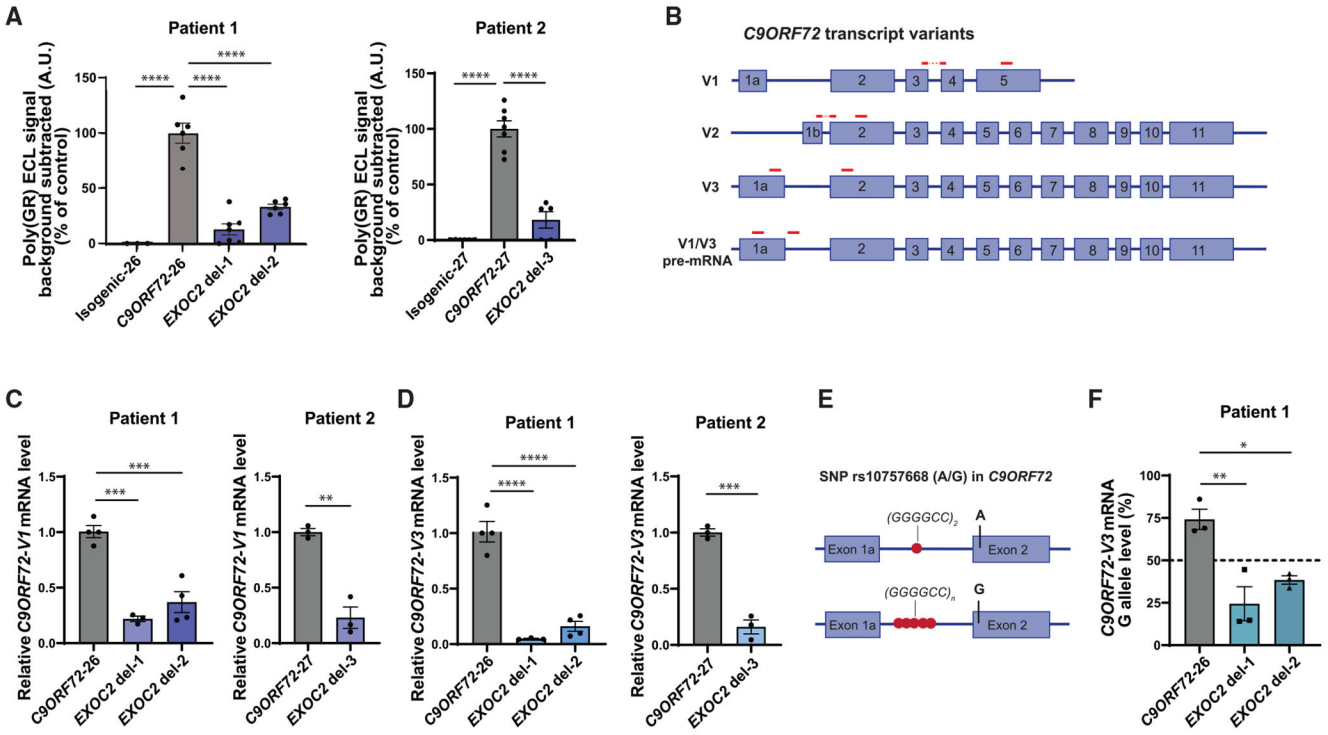


**Figure 3. *EXOC2* deletion reduces poly(GR) and *C9ORF72* mRNA levels**

(A) Poly(GR) level in 2-month-old isogenic control, parental, and *EXOC2*-del *C9ORF72* iPSC-MNs.

(B) Schematic representation of the different *C9ORF72* transcript variants and location of the primer sets used to quantify each transcript.

(C and D) qRT-PCR analysis of relative *C9ORF72*-V1 (C) and *C9ORF72*-V3 (D) mRNA levels in parental and *EXOC2*-del *C9ORF72* iPSC-MNs.

(E) Schematic representation of the location of the (A/G) SNP in *C9ORF72*.

(F) Pyrosequencing quantification of the G allele in *C9ORF72* and *EXOC2*-del iPSC-MNs from one patient. Each data point represents one differentiation ($n$ = 3–6 independent differentiations). Values are mean ± SEM. **$p < 0.01$; ***$p < 0.001$; ****$p < 0.0001$ by one-way ANOVA with Dunnett's multiple comparisons test (A and F and patient 1 in C and D) and two-tailed Student's t test (patient 2 in B and C).

See also Figure S3.

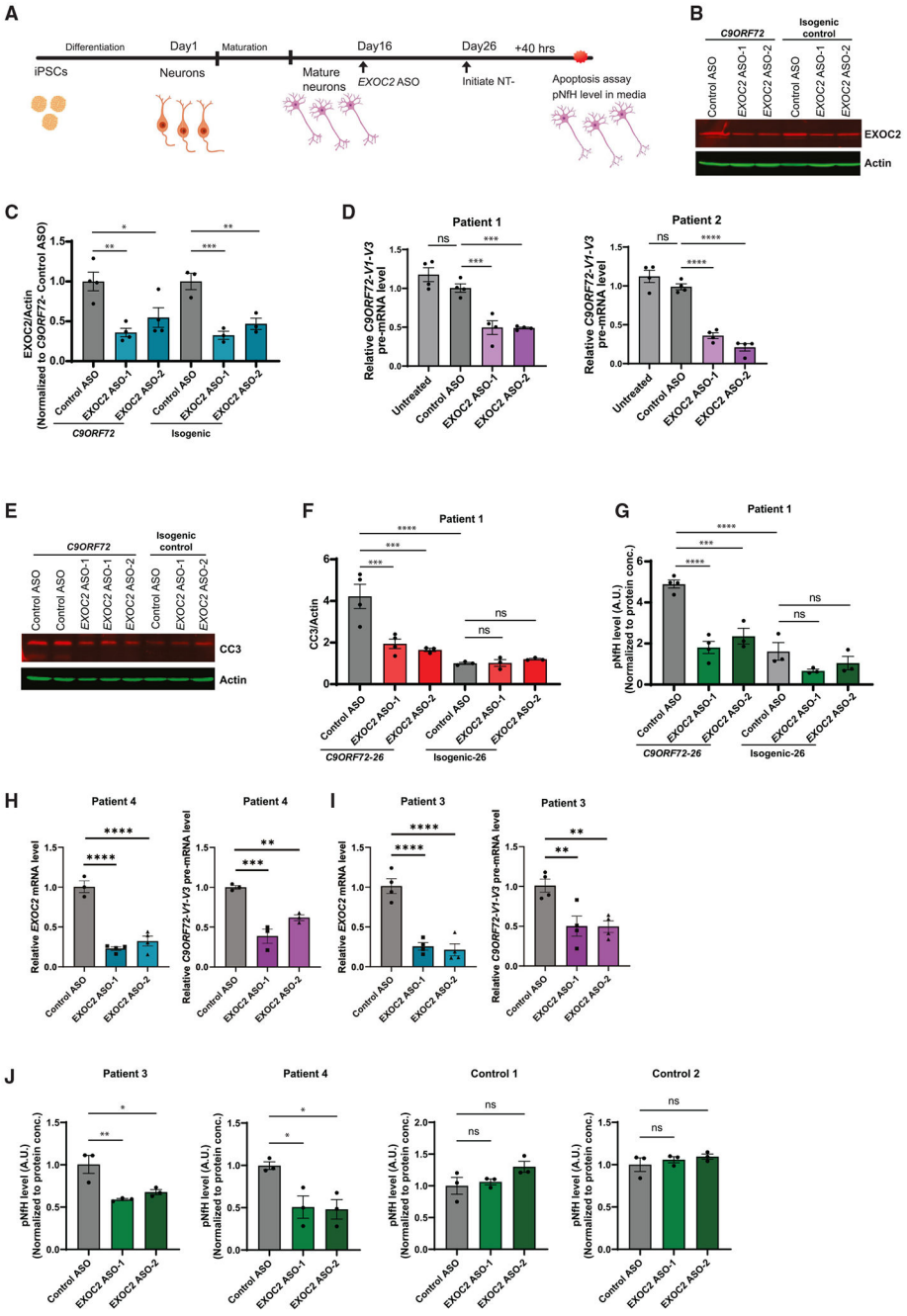


**Figure 4. Treatment of mature iPSC-MNs with *EXOC2* ASOs rescues disease phenotypes**

(A) Schematic of ASO treatment and stress induction in mature iPSC-MNs.

(B) Representative western blot image showing *EXOC2* knockdown efficiency in mature isogenic control or *C9ORF72* motor neurons.

(C) Densitometric quantification of EXOC2 protein levels.

(D) $G_4C_2$ repeats-containing pre-mRNA levels in *C9ORF72* patient neurons treated with *EXOC2* ASOs.

(E and F) Representative western blot image (E) and densitometric quantification (F) of CC3 in mature isogenic control and *C9ORF72* iPSC-MNs treated with control or *EXOC2* ASOs.
(G) ELISA showing pNfH in culture media from mature isogenic control and *C9ORF72* iPSC-MNs treated with control or *EXOC2* ASOs to assess neurodegeneration. pNfH levels were normalized to total protein concentration.
(H and I) qRT-PCR analysis of relative *EXOC2* mRNA and *C9ORF72* V1/V3 pre-mRNA levels in 3-week-old *C9ORF72* patient 4 (H) or patient 3 (I) iPSC-MNs left untreated or treated with 5 μM nontargeting control ASO or *EXOC2* ASOs.
(J) pNfH levels (normalized to total protein concentration) in culture media from mature iPSC-MNs of *C9ORF72* patients and healthy subjects treated with control or *EXOC2* ASOs to assess neurodegeneration. Each data point represents one differentiation ($n = 3–4$ independent differentiations). Values are mean ± SEM. $^{**}p < 0.01$; $^{***}p < 0.001$; $^{****}p < 0.0001$ by one-way ANOVA with Dunnett's multiple comparisons test.
See also Figure S4.

## KEY RESOURCES TABLE

| REAGENT or RESOURCE | SOURCE | IDENTIFIER |
|---|---|---|
| Antibodies | | |
| Rabbit anti-EXOC2 [EPR9420] | Abcam | Cat#ab140620 |
| Mouse anti-β actin | Sigma | Cat#A2228 |
| Mouse anti-MAP2 | Sigma | Cat#M9942 |
| Mouse anti-βIII Tubulin | Promega | Cat#G7121 |
| Rabbit anti-NMDAR 2B | Alomone Labs | Cat#AGC-003 |
| Rabbit anti-Cleaved Caspase 3 (Asp175) | Cell Signaling Technology | Cat#9661 |
| Rabbit anti-SQSTM1/p62 | Abcam | Cat#91526 |
| Mouse anti-SQSTM1/p62 | Sigma | Cat#WH0008878M1 |
| Mouse anti-α Tubulin | Sigma | Cat#T6199 |
| Rabbit anti-$(GR)_8$ | Covance | Custom |
| Anti-$(GR)_8$ GOLD SULFO | MSD | Cat#R31AA |
| Critical commercial assays | | |
| DNeasy Blood&Tissue Kit | Qiagen | 69506 |
| RNeasy Mini Kit | Qiagen | 74106 |
| TaqMan Reverse Transcription Kit | Thermo Fisher Scientific | N8080234 |
| SYBR Select Master Mix | Thermo Fisher Scientific | 4472918 |
| PNFH ELISA Kit | EnCor Biotechnology | ELISA-pNfH-V2 |
| Experimental models: Cell lines | | |
| Human: *EXOC2*$^{-/-}$ *C9ORF72* iPSC line 1 (*EXOC2* del-1) | This paper | N/A |
| Human: *EXOC2*$^{-/-}$ *C9ORF72* iPSC line 2 (*EXOC2* del-2) | This paper | N/A |
| Human: *EXOC2*$^{-/-}$ *C9ORF72* iPSC line 3 (*EXOC2* del-3) | This paper | N/A |
| Human: Isogenic control iPSC line 26Z90 (Control 1) | Lopez-Gonzalez et al.[21] | N/A |
| Human: Isogenic control iPSC line 27M91 (Control 2) | Lopez-Gonzalez et al.[21] | N/A |
| Human: Control iPSC line 2L20 (Control 3) | Almeida et al.[37] | N/A |
| Human: Control iPSC line 37L20 (Control 4) | Zhang et al.[55] | N/A |
| Human: C9ORF72 carrier iPSC line 26L6 (Patient 1) | Almeida et al.[37] | N/A |
| Human: C9ORF72 carrier iPSC line 27L11 (Patient 2) | Almeida et al.[37] | N/A |
| Human: C9ORF72 carrier iPSC line 16L14 (Patient 3) | Lopez-Gonzalez et al.[17] | N/A |
| Human: C9ORF72 carrier iPSC line 40L3 (Patient 4) | Freibaum et al.[56] | N/A |
| Human: C9ORF72 carrier iPSC line 29ALS | Sareen et al.[40] | N/A |
| Experimental models: Organisms/strains | | |
| *D. melanogaster: UAS-(GR)80* | Yang et al.[16] | N/A |
| *D. melanogaster: UAS-GFP* | Yang et al.[16] | N/A |
| *D. melanogaster: w[1118]* | Bloomington Drosophila Stock Center | BDSC:3605 |
| *D. melanogaster*: w[1118]; P{GMR-GAL4.w[-]}2/CyO | Bloomington Drosophila Stock Center | BDSC:9146 |

| REAGENT or RESOURCE | SOURCE | IDENTIFIER |
|---|---|---|
| *D. melanogaster:* w[*]; P{w[+mC] = tubP-GAL80[ts]}20; | Bloomington Drosophila | BDSC:7019 |
| TM2/TM6B, Tb[1] | Stock Center | |
| *D. melanogaster*: y[1] v[1]; P{y[+t7.7] | Bloomington Drosophila | BDSC:27526 |
| v[+t1.8] = TRiP.JF02676}attP2 | Stock Center | |
| *D. melanogaster: y[1] v[1]; P{y[+t7.7]* | Bloomington Drosophila | BDSC:50556 |
| *v[+t1.8] = TRiP.GLC01676}attP2* | Stock Center | |
| Oligonucleotides | | |
| *EXOC2* sgRNAs, see Table S1 | This paper | N/A |
| *EXOC2* PCR primers, see Table S1 | This paper | N/A |
| qRT-PCR primers, see Table S1 | Yuva-Aydemir et al.[31] | N/A |
| *C9ORF72-V3* pyrosequencing primers, See Table S1 | Yuva-Aydemir et al.[31] | N/A |
| Recombinant DNA | | |
| pCAG-eCas9-GFP-U6-gRNA | Deposited by Jizhong Zou | Addgene plasmid # 79145 |
| pCMV delta R8.2 | Deposited by Didier Trono | Addgene plasmid # 12263 |
| pCMV-VSV-G | Stewart et al.[57] | Addgene plasmid # 8454 |
| pLenti CMV GFP Puro (658-5) | Campeau et al.[58] | Addgene plasmid # 17448 |
| Software and algorithms | | |
| ImageJ | NIH | https://imagej.nih.gov/ij/index.html |
| GraphPad | Prism | https://www.graphpad.com/features |
| Zen | Zeiss | N/A |
| ImageStudio | Li-Cor | https://www.licor.com/bio/image-studio-lite/ |